

The Photometric Properties of the *HST* Astrometer Fine Guidance Sensor

B. Bucciarelli^{1,2}, S. T. Holfeltz¹, M. G. Lattanzi^{1,2,3}, L. G. Taff¹
and P. C. Vener-Saavedra^{1,4}

Abstract

This paper presents the results of the photometric calibration of the astrometer Fine Guidance Sensor on the Hubble Space Telescope. Dozens of observations of the 9.58 mag Fine Guidance Sensor TRANSfer Mode reference star Uggren 69 (in the cluster NGC 188) have been utilized to verify the consistency and demonstrate the temporal stability of the photo-multipliers. The measurements which provided the material for a transformation from the FGS instrumental system to the Johnson V magnitude consisted of the extensive POSition Mode observations performed during the Optical Field Angle Distortion calibration. A total of 588 measurements of 92 stars in the galactic cluster M35 were performed. Johnson V band photometry with a precision of $\pm 0.m05$ is available with an accuracy of 0.m05 over two years.

I. Introduction

The issues pertinent to the astrometric calibration of the Hubble Space Telescope Fine Guidance Sensors were discussed by Taff (1990a). Unmentioned in that paper was the photometric calibration of the Fine Guidance Sensors (FGSs). While it may seem superfluous to do 1 percent photometry from a space-based platform, in fact the small amplitude variability of one star has already been re-discovered with the astrometer Fine Guidance Sensor (Benedict et al. 1993). Moreover, with the removal of the High Speed Photometer from the *HST* to make room for the Corrective Space Telescope Axial Replacement (COSTAR), the Fine Guidance Sensors, with their 25 milli-second time resolution, become the fastest photometric devices on the observatory. This too has already borne fruit with the observation of a \sim hundred milli-second flare (Benedict et al. 1993). Therefore, there is scientific value to what is a secondary calibration of the FGSs.

Despite the spherical aberration in the primary mirror of the Optical Telescope Assembly (OTA) (Burrows et al. 1991) and the eventual recognition of the fact that each FGS has a unique set of optical and mechanical problems, the photometric performance of the FGSs has apparently not been affected. We believe this to be so because their entrance aperture is 5 x 5 arcsec (albeit degraded as a result of field stop mis-alignments). Moreover, the introduction of COSTAR will not change the

-
1. Space Telescope Science Institute, Baltimore, MD 21218
 2. On leave from Torino Observatory.
 3. Affiliated with the Astrophysics Division, Space Science Department, ESA.
 4. Now with Advanced Computer Concepts, GSFC.

nature of the wave front received by the FGSs for they are located in radial bays at the perimeter of the focal plane. Hence, the photometric behavior of the FGSs is not expected to change in the foreseeable future. One major change from the original scientific calibration plan for the FGSs is that instead of performing observations designed to calibrate all three, only one FGS (the astrometer) is being scientifically metered. This is the one in radial bay #3 and not the one in radial bay #2, which was the pre-launch expectation. The FGS in radial bay #2 evinces the worst performance with the deformed primary mirror and the pre-COSTAR positioning of the secondary mirror of the OTA. The FGSs in radial bays #1 and #2 will only partake of the general engineering calibrations for the FGSs.

Below we first discuss the stability of the photo-multipliers in the astrometer FGS. After demonstrating ± 0.01 mag level performance over the last year and one-half, we then turn to the photometric calibration of the collective action of the four photo-multipliers in the astrometer FGS. We have used the measurements acquired for completion of the Optical Field Angle Distortion—one of the two principal calibration activities for positional astrometry—to provide the information necessary to construct a photometric calibration of the astrometer FGS. Providing a transformation from the FGS instrumental system to a standard photometric system for each of the photo-multipliers separately is a less interesting task because all four PMTs are always in use. However, the sensitivity and responsivity mis-matches between the two photo-multipliers on each axis of an FGS are of engineering and scientific concern so this issue is addressed herein. Several papers dealing with various aspects of the Fine Guidance Sensors have been published (e.g. Taff 1990b, 1991, Bradley et al. 1991). The reader is directed to them for a discussion of the electro-optical aspects of the Fine Guidance Sensors and their intended engineering and scientific functions. Scientific data reduction for the FGSs is discussed in Lattanzi et al. (1992 and 1993).

II. Stability of the Photo-multipliers

To evaluate the temporal stability of the FGS photo-multipliers we have utilized many measurements of the same star since launch. Because the spherical aberration ruined the anticipated collimation of the OTA, an extended empirical attempt to find the optimal positioning of the secondary mirror was carried out. A series of “Nine Points of Light” tests and “Five Points of Light” tests were conducted during the collimation phases of the *HST* commissioning. The same star, which we refer to as Upgren 69 (Upgren, Mesrobian & Kerridge 1972), has been used for all of them. This star has also been used in various engineering and scientific calibrations (principally TRANSfer Mode). Hence, as a consequence of its frequent observation, this star has become the reference star for FGS TRANSfer Mode observing. This star is apparently single—as far as can be determined from FGS observations—point-like, and unvarying in brightness. From the Upgren et al. reference, its V magnitude is 9.58 and its B – V color index is 0.50. The results for the most recent 1.5 years are summarized in Figure 1.

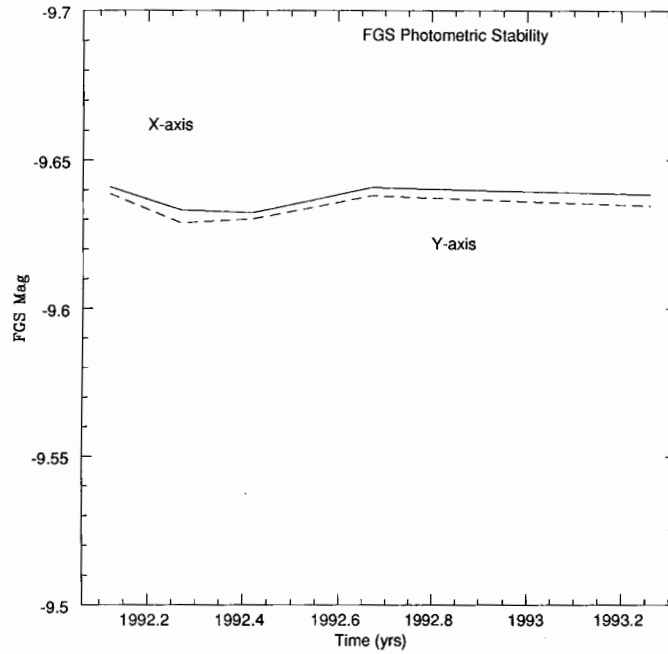


Figure 1: Time history of the astrometer FGS measurements of Upgren 69.

III. Photometric Calibration Data

iii.i Reference Star Data

There is one source of photo-electric photometry of M35 in the literature, Hoag et al. (1961). This work also includes extensive photographic photometry so we adopt it as our reference standard. Additional photographic photometry of this galactic cluster by Cudworth (1971), McNamara & Sekiguchi (1986), and Vidal (1973) was brought onto the Hoag et al. system by the one-dimensional version of the infinitely overlapping circles method (Taff, Bucciarelli & Lattanzi 1990; Bucciarelli, Taff & Lattanzi 1993). To see how this method works to minimize the systematic differences between two different sets of V magnitudes, concentrate on one star in both the Hoag et al. and (say) Cudworth lists. We find all the stars also in this intersection set within $\pm \Delta V$ ($\Delta V = 0.^m33$) of its V magnitude and store the individual differences $\delta V = V_{Hoag} - V_{Cudworth}$. These are then averaged together with the infinitely overlapping line weight function $w(z)$;

$$w(z) = 1 - z, z = |\delta V| / \Delta V.$$

Thus, the amount of the adjustment is given by

$$\varepsilon_V = \sum w(z) \delta V / \sum w(z),$$

where the sums are over all the stars in both the Hoag et al. and the Cudworth data sets and within ΔV of the V magnitude of this star. The re-normalization by the sum of the weights is required because $w(0) = 1$. Thus, the value we use for the V magnitude of this star is $V_{Cudworth} + \varepsilon_V$.

In a similar fashion we separately brought the different B – V values onto the Hoag et al. system (this time with a 0.^m08 width). Unfortunately, the Cudworth (1971) color indices showed too much dispersion (and residual systematic tendencies) to be successfully merged with the Hoag et al. values. A separate investigation of the B values and the B – V values vs. V was also undertaken to explore the possibility of more subtle systematic problems as a function of color index. No additional causes for rejection or suspicions of inhomogeneity were found at first. All the remaining V and B – V data, adjusted as described, were then used for the photometric calibration of the astrometer FGS. Having minimized the systematic differences, the weight assigned to the photometry was based on the estimates of the random errors assigned by the authors. After this stage of the analysis was completed it became clear to us that the McNamara & Sekiguchi (1986) data had to be rejected because, relative to the FGS instrumental magnitudes, it too showed subtle color index dependent systematic errors. (While the infinitely overlapping circle can remove systematics at any wavelength, it is imprudent to use it on extremely large scales.) Thus, our actual transformation formulas from the FGS instrumental system to the Johnson V magnitude is based on the Hoag et al. (1961) and Vidal data (1973).

iii.ii Observational Data

The Optical Field Angle Distortion calibration (colloquially known as the OFAD) is designed to correct for the residual distortions induced by the combined Optical Telescope Assembly (i.e., the primary and secondary mirrors of the *HST*) and Fine Guidance Sensor optical system aberrations. The observations to support it were successfully carried out over 20 orbits in early January, 1993. Using experience gained from other FGS observing efforts, the Space Telescope Astrometry Team (led by W. H. Jefferys, Univ. of Texas at Austin) was cleverly able to fit in as many as 30 stars per orbit in a complex measurement sequence. Hence, 588 POSition Mode measurements of 92 different stars, in the galactic cluster M35, were obtained.

IV. Numerical Results

iv.i Dead-Time Corrections

The formula for the correction from measured counts (M_C) per unit of integration time (typically 25 msec for the FGSs) to true counts (T_C) is (Hubble Space Telescope Astrometry Operations Handbook 1986, pg. 3-73)

$$T_C/M_C = 1/[1 - M_C(\delta T/\tau)], \quad (1)$$

where δT is the dead-time constant (285 nanoseconds) and τ is the integration time. Equation (1) is expressed on a magnitude scale by taking the common logarithm of the ratio T_C/M_C . Figure 2a shows the amount of correction (in magnitudes) owing to the photo-multiplier dead-time which needs to be applied to the instrumental magnitudes (as derived from the measured counts) as a function of visual (Johnson) magnitude. The absolute throughput (counts) is that for the F583W (Clear) filter. For example, for our standard single star Uppgren 69 (V = 9.^m58) the dead-time correction amounts to 0.09 mag.

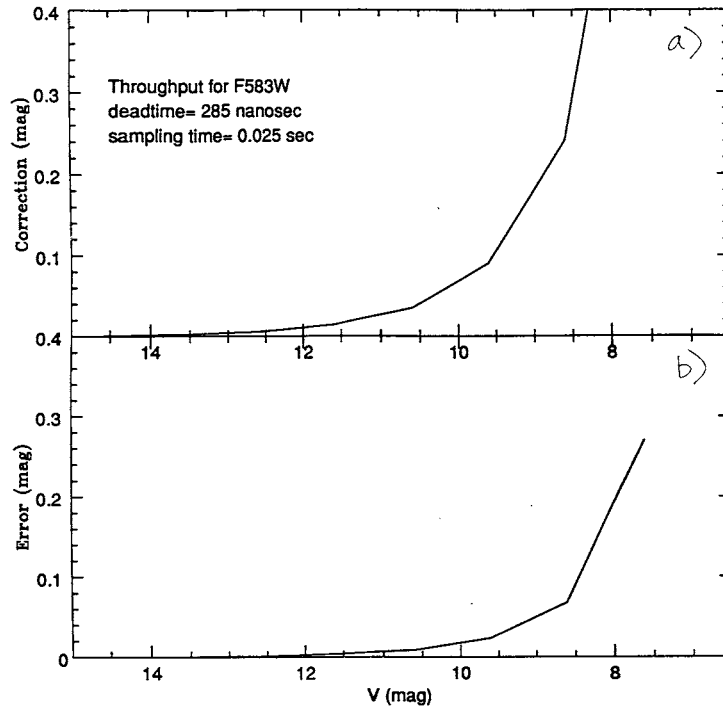


Figure 2: a) Plot of the dead-time correction as a function of V magnitude. b) Graph of the error in the dead-time correction with a 25 percent uncertainty in the dead-time constant.

The dead-time constant just given is based on pre-launch measurements. There has been no in-flight calibration of the dead-time constant either during the Orbital Verification or Science Verification phases of operation. In Eq. (1), the measured counts are known to the limit of the photon noise, while τ is a given number. Thus, an error in the adopted value for the dead-time constant will show as an error in the predicted correction derived from Eq. (1). This error is (in dex)

$$\sigma_{\Delta m} = [2.5 \log e \times 10^{0.4 \Delta m} M_C (\delta T / \tau)] \sigma_{\delta T} / \delta T, \quad (2)$$

where $\sigma_{\Delta m}$ is the error of the correction Δm as derived from Eq. (1) (after conversion to a magnitude scale) and $\sigma_{\delta T}$ is the error of the dead-time constant. In Figure 2b we show a plot of Eq. (2) as a function of magnitude for an assumed error in the dead-time constant of 25 percent.

From the two figures we conclude that the dead-time correction is important enough to be routinely removed from the data (and this feature is now built into the Institute's astrometry data processing software). The contribution from our uncertainty in the dead-time constant is several times less than the sought for correction (the actual errors probably being smaller than that depicted in Figure 2b).

iv.ii Linearity

We start out assuming that the relationship between FGS magnitude, m_{fgs} , the mean value of the measured counts, $\langle C \rangle$, and color index, $B - V$, is of the form

$$m_{fgs} = -2.5 \log \langle C \rangle, \text{ and } V = -2.5 \log \langle C \rangle + \alpha + \beta (B - V),$$

where α and β are constants to be determined. In fact, at first we considered a more general model with the numerical factor of 2.5 in the m_{fgs} formula replaced by another constant (say 2.5γ). After extensive testing, not further described herein, we were convinced that the value of this constant was in fact unity ($\gamma = 1.0000 \pm 0.0001$). Hence, we assumed it from that point on.

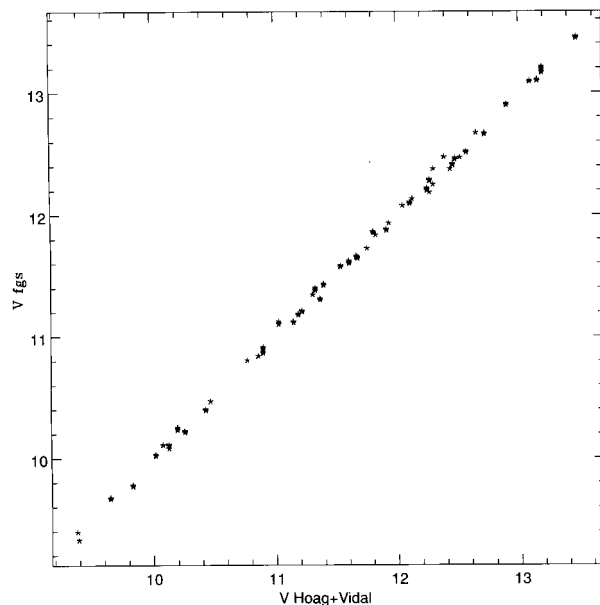


Figure 3: Corrected FGS V magnitude plotted against the standard V magnitude (i.e., the weighted average of the Hoag and Vidal photometry). Note that the 45°, zero intercept line is followed.

Fits [using the GAUSSFIT software (Jefferys 1988)] without the color index term were noticeably poorer than those with it. This is not surprising in view of the wide pass-band of the F583W filter (i.e., 2400Å). Finally, as indicated above, tests of the results after the fit demonstrated that the McNamara & Sekiguichi (1986) data was contaminated by a color index dependent systematic error. Therefore, we eliminated it from our pool of reference data and executed the least squares fits once more relying only on the Hoag et al. (1961) and Vidal (1973) measurements. Graphical results are presented in Figures 3–6. The numerical values of α and β were determined to be 20.060 ± 0.003 and -0.164 ± 0.010 respectively.

From the size of β it is clear that there exists a non-trivial color index dependence in the instrumental FGS magnitude (i.e., in m_{fgs}). However, its amplitude is small and knowing an approximate value of $B - V$, say even to $\pm 0.^m25$, is sufficient to continue to do at least 5 percent photometry.

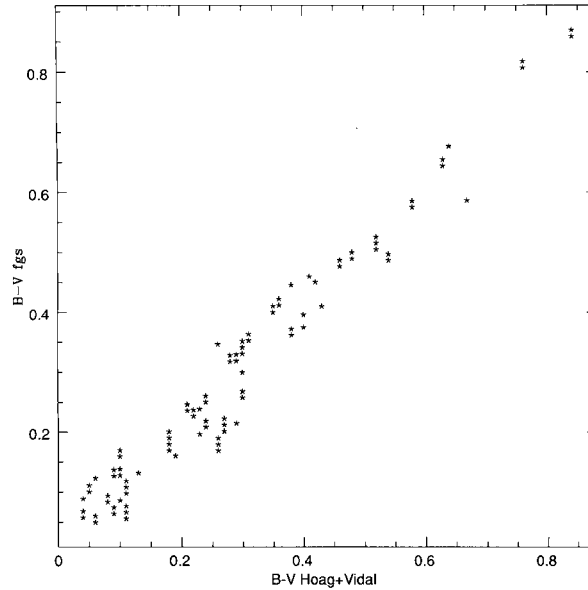


Figure 4: Corrected FGS B - V color index plotted against the standard B - V color index (i.e., the weighted average of the Hoag and Vidal photometry). Note again that the 45°, zero intercept line is followed.

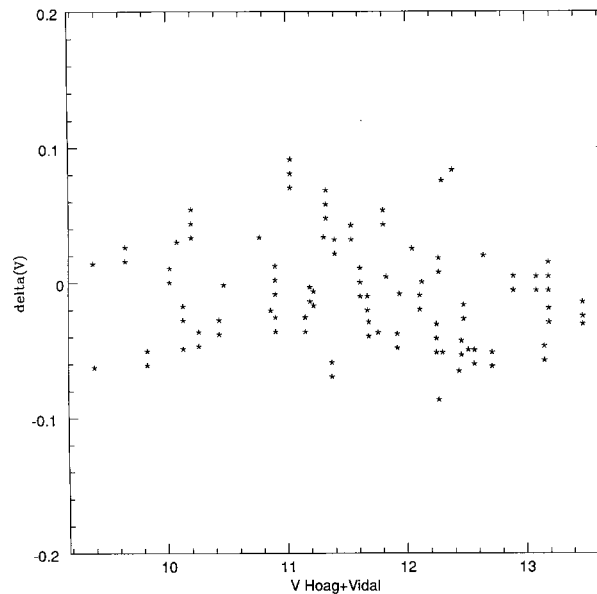


Figure 5: The difference between the FGS V magnitude and the standard V magnitude plotted against the standard V magnitude (i.e., the weighted average of the Hoag and Vidal photometry). Observe that there is no bias and an absence of systematic trends.

iv.iii Photomultiplier Tube Bias per Axis

Using all the observations of the Optical Field Angle Distortion POSITION Mode measurements, we have evaluated the differences between the two photo-multipliers per FGS interferometer axis. (These are usually referred to as the x and y axes and the two photo-multipliers as the A and B PMTs.) The results are plotted in Figures 7 and 8. There is evidence of a small color index dependent effect and clearly the two Y axis photo-multipliers are unbalanced.

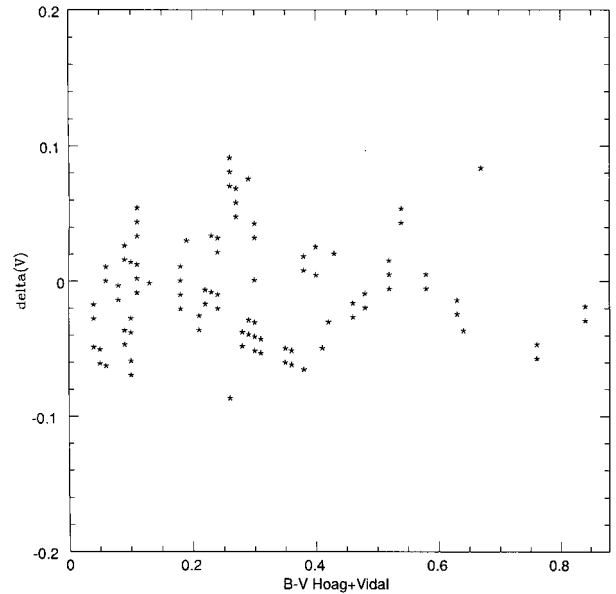


Figure 6: The difference between the FGS V magnitude and the standard V magnitude plotted against the standard B – V color index (i.e., the weighted average of the Hoag and Vidal photometry). Observe again that there is no bias and an absence of convincing systematic trends.

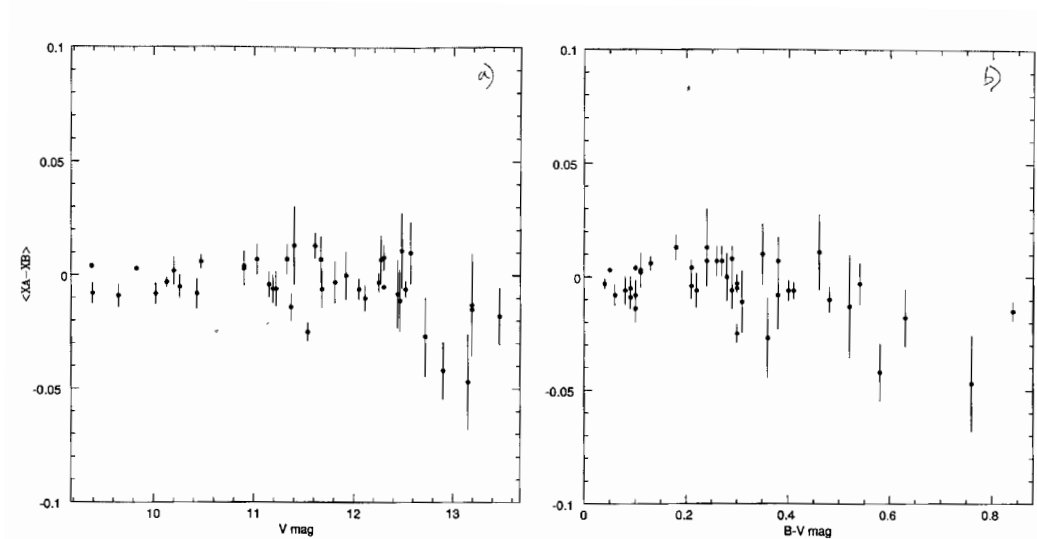


Figure 7: a) X axis count differences, expressed as a magnitude, vs. V magnitude. The error bars indicate the standard deviation about the mean of repeated observations of the same star. b) X axis count differences, expressed as a magnitude, vs. B – V color index, as in Figure 7a.

Conclusions

We have described the methods and material used to ascertain the temporal stability of the astrometer Fine Guidance Sensor photo-multiplier tubes. After satisfying ourselves of this fact we have similarly presented the data and analysis techniques used to photometrically calibrate this device. With a 25 milli-second time resolution, the FGS photo-multipliers are the best means of obtaining fast photometry from *HST*.

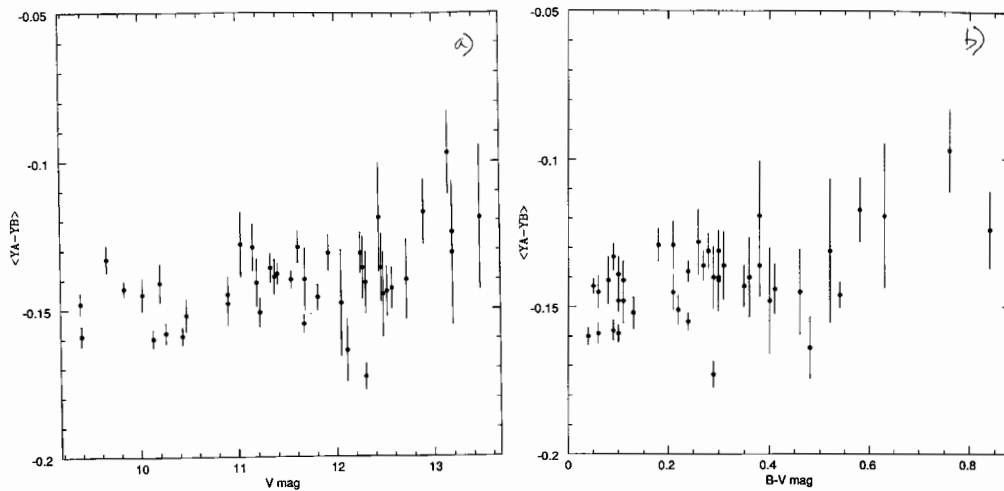


Figure 8: a) Y axis count differences, expressed as a magnitude, vs. V magnitude, as in Figure 7a. Note the non-trivial offset from a null value. b) Y axis count differences, expressed as a magnitude, vs. B - V color index, as in Figure 7a.

This work was partially supported by NASA Grants NAGW-2597 and CW- 0016-92.

References

- Benedict, F., E. Nelan, B. McArthur, D. Story, W. van Altena, Yang Ting-gao, W. H. Jefferys, P. D. Hemenway, P. J. Shelus, A.L. Whipple, O. G. Franz, L.W. Fredrick, and R. L. Duncombe, 1993, *PASP*, 105, 487
- Bradley, A., Abramowicz-Reed, L., Story, D., Benedict, G., and Jefferys, W., 1991, *PASP* 103, 317.
- Bucciarelli, B., Taff, L. G., and Lattanzi, M. G., 1993, *J. Statist. Comput. Simu.* 48, 29
- Burrows, C. J., Holtzman, J. A. Faber, S. M. Bely, P. Y., Hasan, H., Lynds, C. R., and Schroeder, D., 1991, *ApJ* 369, L21
- Cudworth, K. M., 1971, *AJ* 76, 475
- Hoag, A. A., Iriarte, B., Johnson, H. L., Hallan, K. L., Mitchell, R. I., and Sharpless, S., 1961, *Publ. U. S. Naval Obs. Rep.* 17, 349
- Jefferys, W. H., Fitzpatrick, M. J., McArthur, B. E. and McCartney, J. E., 1988, *GaussFit: A System for Least Squares and Robust Estimation USER'S MANUAL*, Version 1.0, (Univ. Texas at Austin, Dept. of Astronomy and McDonald Obs.)
- Lattanzi, M. G., Bucciarelli, B., Holfeltz, S. T., and Taff, L. G., 1992, "The Analysis of *HST* Fine Guidance Sensor Transfer Functions," in *Complementary Approaches to Double and Multiple Star Research*, eds. H. A. McAlister and W. I. Hartkopf, ASP, San Francisco, pg. 377
- Lattanzi, M. G., Bucciarelli, B., Holfeltz, S. T., and Taff, L. G., 1993, "Astrometry with the *HST* Fine Guidance Sensors," in *Developments in Astrometry and Their Impact on Astrophysics and Geodynamics*, eds. I. I. Mueller and B. Kolaczek, Dordrecht, The Netherlands, pg. 47

- McNamara, B. and K. Sekiguchi, 1986, AJ 91, 557
Taff, L. G. 1990a, ApJ 365, 407
Taff, L. G. 1990b, Exp. Astr. 1, 237
Taff, L. G. 1991, Adv. Sp. Res. 1, 97
Taff, L. G., Bucciarelli, B., and Lattanzi, M. G., 1990, ApJ 361, 667
Vidal, N. V. 1973, A&A Suppl. 11, 93
Uggen, A. R., Mesrobian, W. S., and Kerridge, S. J., 1972 AJ, 77, 74